Available online at www.sciencedirect.com
SCIENCE DIRECT®
Aerosol Science 36 (2005) 1322–1337
Journal of Aerosol Science
www.elsevier.com/locate/jaerosci

Pressure-dependent efficiency of a condensation particle counter operated with FC-43 as working fluid

M. Hermann[a,*], S. Adler[a], R. Caldow[b], F. Stratmann[a], A. Wiedensohler[a]

[a] *Leibniz-Institute for Tropospheric Research, Physics Department, Permoserstr. 15, 04318 Leipzig, Germany*
[b] *TSI Incorporated, Shoreview, Minnesota, USA*

Received 12 November 2004; received in revised form 9 February 2005; accepted 1 March 2005

Abstract

The counting efficiency of the TSI CPC 7610 operated with FC-43 as working fluid was investigated for three temperature differences in the pressure range 60–1000 hPa. At the standard temperature difference of 17 K, the CPC threshold diameter decreases from 20 to 11.5 nm and the maximum counting efficiency increases from ∼ 30% to ∼ 100% as the operating pressure is reduced from 1000 hPa down to 60 hPa. Calibration with NaCl and H_2SO_4 particles indicates that the counting efficiency depends on particle material. Comparing the results with butanol curves shows that butanol yields above 200 hPa more stable counting efficiency curves with lower threshold diameters and higher maximum counting efficiencies. However, below 200 hPa, FC-43 shows the better performance and can be used at least down to 60 hPa. Computational fluid dynamics modelling was carried out to explain some of the observed differences.

Keywords: Particle counter; Low-pressure operation; FC-43

1. Introduction

Condensation Particle Counters (CPCs) of the conductive-cooling-type are widely used in particle measurements (Willeke & Baron, 2001). Inside these counters, the sampling aerosol is first saturated with a working fluid in the saturator. Downstream the saturator, the aerosol is cooled in the condenser and the particles begin to grow by condensation of the supersaturated working fluid. The enlarged particles are

* Corresponding author. Tel.: +49 341 235 2918; fax: +49 341 235 2361.
E-mail address: hermann@tropos.de (M. Hermann).

0021-8502/$ - see front matter © 2005 Elsevier Ltd. All rights reserved.
doi:10.1016/j.jaerosci.2005.03.002

finally detected by light scattering in a laser optics. CPCs are normally characterised by their counting efficiency, which is defined as the ratio of the particle number concentration counted by the CPC to the given particle number concentration. To describe the counting efficiency curve, usually a lower particle size detection limit, the threshold diameter, and the asymptotic maximum counting efficiency for particles much larger than the threshold diameter are used. The physical properties of the working fluid, such as the vapour pressure or the diffusion coefficient, determine the counting efficiency of the CPC at given operating pressure, volume flow rate, and temperature difference between the saturator and the condenser. Most of the commercial CPCs use alcohol, in particular butanol, as a working fluid. However, there are applications where it is necessary to employ a different working fluid. This can be the case if it is desired to operate the CPC in a pressure or particle size range which cannot be accessed with butanol. For example, for the TSI CPC 7610 (TSI Inc., St. Paul, MN, USA), Hermann and Wiedensohler (2001) have shown that the application range of the instrument with butanol is limited to operating pressures larger than 160 hPa. Another reason can be safety regulations, because butanol is highly flammable and might not be allowed in certain environments, such as aboard an aircraft.

In the present study, we extend our former investigation on three modified TSI CPCs 7610 (cf. Hermann & Wiedensohler, 2001) by using a perfluorinated organic compound, perfluorotributylamin ($C_{12}F_{27}N$ or FC-43, 3M, St. Paul, MN, USA) as working fluid. Fluorocarbons were already used as working fluids in CPCs (e.g., Keady, Denler, Sem, Stolzenburg, & McMurry, 1988; Brock et al., 2000; Hanson, Eisele, Ball, & McMurry, 2002), however, for commercial CPCs there are nearly no counting efficiency data reported in the literature. In this study, we present counting efficiency curves of the CPC 7610 operated with FC-43 at three temperature differences (11, 17, and 26 K) in the pressure range from 60–1000 hPa. The response of the counter to different particle material was investigated by using NaCl and H_2SO_4 particles for calibration. The FC-43 curves are compared to former calibration results obtained with butanol. In order to interpret the results, we used a computational fluid dynamics (CFD) code (FLUENT) in combination with the fine particle module (FPM, Particle Dynamics, 2003) to calculate the FC-43 saturation in the CPC saturator block.

2. Experimental

The set-up used for the CPC 7610 calibration is shown in Fig. 1 (Adler, 2003). Polydisperse sodium chloride (NaCl) aerosol was generated in a tube furnace at temperatures of 510–560 °C (Fig. 1a), according to Scheibel and Porstendörfer (1983). Therefore, we used compressed air with RH smaller than 3% for all indicated flows. For the sulphuric acid particles, a 0.1% solution of sulphuric acid and highly purified water was nebulised in an atomiser (TSI Model 3076, TSI Inc., St. Paul, MN, USA). The generated particles were dried in a diffusion dryer (Fig. 1b) and then re-evaporated in a tube furnace (140 °C), to form pure sulphuric acid particles by homogeneous nucleation (Saros, Weber, Martri, & McMurry, 1996). A citric acid filter was located in the trunk line of the compressed air to remove ammonia from the gas stream and thereby to prevent neutralisation of the sulphuric acid particles. Hanson et al. (2002) report that ammonia concentrations of 1-2ppbV are already sufficient to neutralise sulphuric acid particles in a tubing system. The conditions in our set-up were in a range, where they observed a different CPC response to pure sulphuric acid particles and neutralised sulphuric acid particles (i.e., water partial pressure < 6.5 hPa and particle diameters > 4 nm). However, the citric acid filter we used in our set-up should have removed most of the ammonia in the compressed air and the long run-up time of the system of about one hour

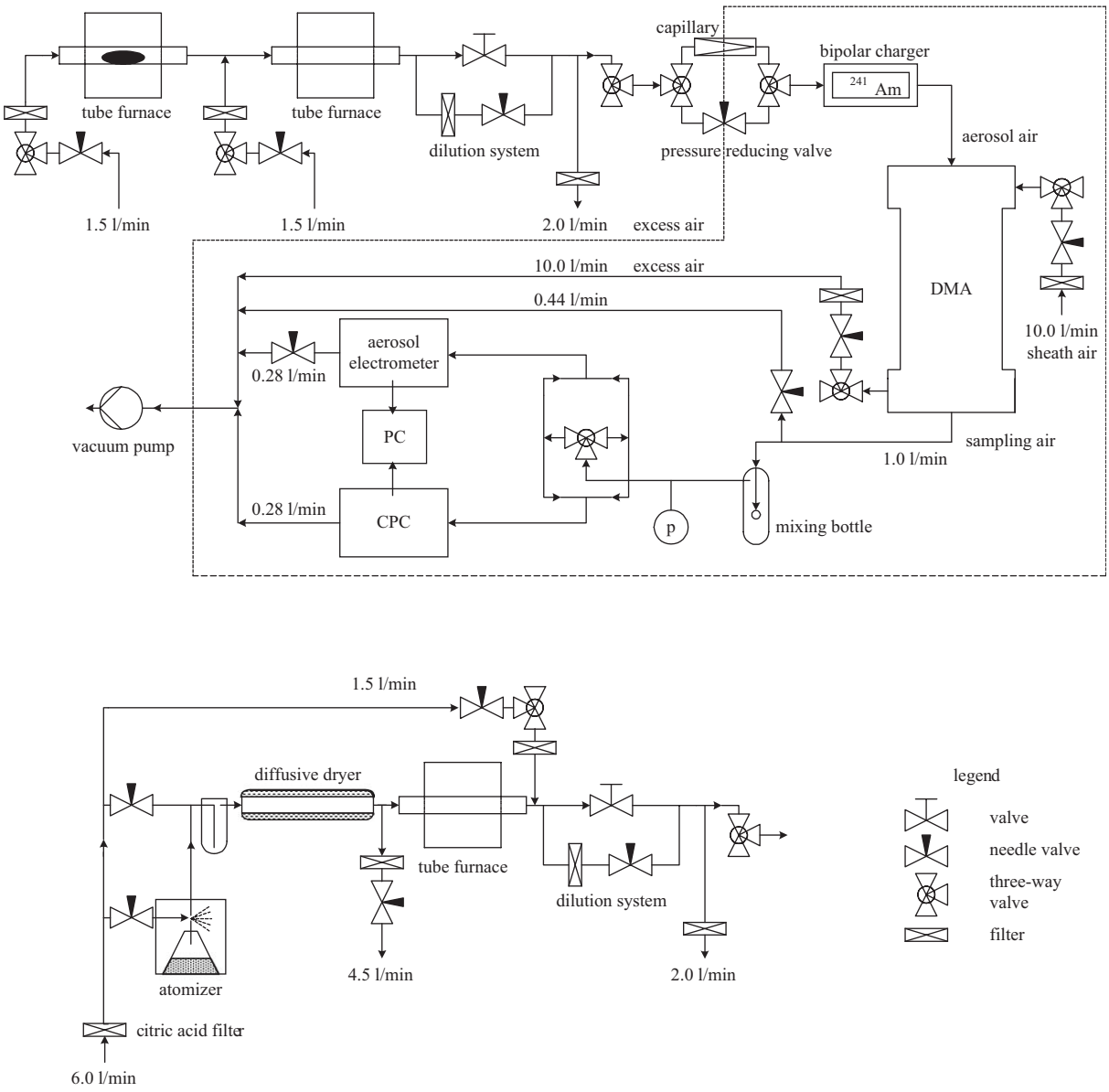

Fig. 1. CPC 7610 calibration set-up. Indicated flow rates are given at STP for the 200 hPa setting.

should have helped to remove possible ammonia from surfaces in the set-up. Hence, we assume that we measured pure sulphuric acid particles.

Downstream of a dilution system, the pressure in the set-up was reduced from ambient conditions to the operating pressure (60–1000 hPa) using a needle valve or a glass capillary as restrictor. For each operating pressure and given flow rate a capillary was manufactured. Downstream of the capillary, the aerosol was charged in a ^{241}Am bipolar charger and a quasi monodisperse fraction of the aerosol was selected by a differential mobility analyser (DMA, Hauke type, short: $L = 11\,\text{cm}$, $r_{\text{inner}} = 2.5\,\text{cm}$, $r_{\text{out}} = 3.35\,\text{cm}$).

The DMA was operated with flow rates of 1 and 10 l/min (STP) for the aerosol and sheath air flow, respectively. First the aerosol and sampling flow rates were applied to the DMA and the operating pressure in the DMA was reduced to the desired value. The sheath and excess air flow rates were set by needle valves and measured at ambient pressure. Afterwards three-way valves were switched simultaneously to pass the respective flows into or out of the DMA. Downstream the needle valves the set flows now expanded to larger flow rates at the lower operating pressure inside the DMA. This course of action is valid because the relationship between the particle diameter and the applied voltage does not change with pressure in the free molecular regime (cf. Seto et al., 1997). Comparison between counting efficiency curves obtained with the DMA operated at 200 and 1000 hPa, respectively, confirm this assumption. At the lowest operating pressure (60 hPa), the DMA flow rates had to be reduced to 0.4 and 4 l/min (STP), respectively, because the suction rate of the pump was not sufficient to maintain higher flow rates. Downstream of the DMA, a mixing bottle was installed to assure that the monodisperse aerosol leaving the DMA was distributed homogeneously over the transport line. With a three-way-valve system upstream of the CPC, the spatial homogeneity of the aerosol was regularly checked, by swapping the CPC and aerosol electrometer (AE) flows.

The CPC counting efficiency, η, was obtained by comparing the particle number concentration measured by the CPC with the reading of the AE. Thereby, the time and pressure dependent AE-offset had to be considered, whereas the error due to multiple charged particles could be neglected compared to other experimental errors (Adler, 2003). Systematic differences in CPC and AE readings were minimised by using two transport lines of equal length and geometry, as well as the same flow rate through both lines. This flow rate was given by the critical orifice of the CPC and was measured as function of operating pressure to be 1.1–1.6 l/min. Particle signals of the CPC and the AE were recorded by a multifunction data acquisition card (counter and analogue input) in a PC. The counting efficiency curves shown in the following section represent the mean values of three curves measured for each operating pressure and temperature difference in the CPC.

3. CFD Model

In order to interpret the differences in the counting efficiencies obtained with butanol and FC-43 (cf. Section 4.4), we modeled the mass transfer inside the CPC 7610 saturator for both working fluids. Therefore, the original CPC 7610 geometry was provided by TSI as file in STEP format. The geometry was imported into GAMBIT (v.2.1.2, Fluent Inc., Lebanon, NH, www.fluent.com) and a 3D 180 °-mirror-symmetric tetrahedral mesh with 3D boundary layer and ∼300,000 grid cells was generated. For the flow field calculation, we used the CFD code FLUENT (v.6.1.22, Fluent Inc., Lebanon, NH, www.fluent.com) in combination with the fine particle module (FPM, Particle Dynamics, 2003, particle dynamics GmbH, Leipzig, www.particle-dynamics.de, Wilck, Stratmann, & Whitby, 2002) to calculate the saturation profiles. The FPM is a commercially available Eulerian model that describes particle–gas and particle–particle interactions and simulates the spatial and temporal evolution of the particle size distribution. It is a user-defined functions (UDFs) based add-on-module to FLUENT 6. For our simulations, the initial particle concentration was set to zero and all particle processes were deactivated. Although we did not use the main features of the FPM here, i.e., to model particle dynamics, this module still offers advantages when dealing with the gas phase alone. The saturation of a compound can be directly set and displayed, without calculating vapour pressures as the respective UDFs already exist. For our

calculations, the saturation of the working fluid at the entrance of the CPC (3/8″ tube) was set to zero, while it was unity at the saturator block walls. As the CPC 7610 controls only the temperature difference between the saturator and the condenser, the absolute temperature of the saturator is not fixed. Monitoring the saturator temperature yielded a difference of less than two degrees between the saturator and its environment (for the standard temperature difference of 17 K). Hence, heat transfer in the saturator could be neglected for the model calculations. All calculations presented here were performed at one saturator temperature, 298 K, because within the range of possible temperatures the CPCs experience during airborne measurement the influence of the temperature on the mean saturation in the saturator is small ($< 2\%$). This was confirmed by a comparison model run at 303 K.

Most of the physical properties of FC-43 and some of butanol had to be estimated using approximation methods. The respective values and references are given in Table 1. For the mixture of air with butanol/FC-43 the *incompressible-ideal-gas* law was chosen for calculating the density, the *mixing-law* for the heat capacity, and the *ideal-gas-mixing-law* for the thermal conductivity and the viscosity. The mass diffusivity was given by the respective diffusion coefficient of butanol/FC-43 in air.

For the model calculations we used the double precision segregated solver in FLUENT. Model runs were carried out both with a *laminar* and a *realisable k-ε turbulence* model with *enhanced wall treatment* (i.e., wall boundary layer explicitly modelled). However, as the difference between the two models in the mean FC-43 saturation at the saturator exit is only 1.2% at 1000 hPa (and probably lower for lower operating pressures because of smaller Re numbers), for the sake of computing time we applied only the laminar model for the other operating pressures.

4. Results and discussion

4.1. Pressure dependence

The CPC 7610 counting efficiency curves for seven operating pressures between 60 and 1000 hPa are shown in Fig. 2. All curves were obtained with the standard temperature difference of 17 K and NaCl particles. Error bars on the x-axis represent one standard deviation of the DMA transfer window (theoretical values, cf. Stolzenburg, 1988) and the y-axis error bars give the experimental standard deviation of the counting efficiency mean values. The upper graph in the figure (Fig. 2a) depicts only five curves to illustrate the influence of the operating pressure on the counting efficiency. For the sake of clarity, the curves for the lowest four pressures are shown in a separate diagram for a smaller diameter range (Fig. 2b).

As shown in Fig. 2, the counting efficiency of the CPC 7610 with FC-43 shifts towards smaller diameters as the pressure is reduced. In the range 60–150 hPa, the instrument has the best performance and reaches the smallest detectable particle diameters (50% particle detection efficiency at 11–12 nm). Likewise, the maximum asymptotic counting efficiency, $\eta_{\max}$ increases from $\sim$ 30% at 1000 hPa to $\sim$ 100% around 100 hPa as the pressure is reduced. These changes in the counting efficiency curve are consistent with results from former studies (cf. Hermann & Wiedensohler, 2001 and references therein), however they are more pronounced than for butanol. The reason for this difference will be discussed in Section 4.4.

4.2. Temperature dependence

CPC 7610 counting efficiency curves for three temperature differences (11, 17, and 26 K) and two operating pressures (200 and 700 hPa) are shown in Fig. 3. These data were obtained using H_2SO_4

Table 1
Physical properties of butanol and FC-43 at 1013 hPa and 298 K

		FC-43		Butanol	
Property	Dimension	Value	Ref.	Value	Ref.
Molecular weight	g/mol	671	http://webbook.nist.gov/chemistry/	74.12	http://webbook.nist.gov/chemistry/
Gas heat capacity	J/kg K	771.5	Joback and Reid, 1987	1456.9	http://webbook.nist.gov/chemistry/
Vapour pressure	Pa	190	http://www.3m.com	8.75	http://webbook.nist.gov/chemistry/
Gas viscsity	kg/m s	8.89e − 6	Lucas, 1984	6.94e − 6	Lucas, 1984
Gas thermal conductivity	W/K m	0.141	Roy and Thodos, 1968, 1970	0.269	Roy and Thodos, 1968, 1970
Diffusion coefficient in air	m^2/s	$3.287e-6\,\frac{1013}{p}$	Fuller and Giddings, 1965; Fuller, Schettler, and Giddings, 1966; Fuller, Ensley, and Giddings, 1969	$8.948e-6\,\frac{1013}{p}$	Fuller and Giddings, 1965; Fuller et al., 1966, 1969

The diffusion coefficient for different operating pressures can be calculated applying p in hPa.

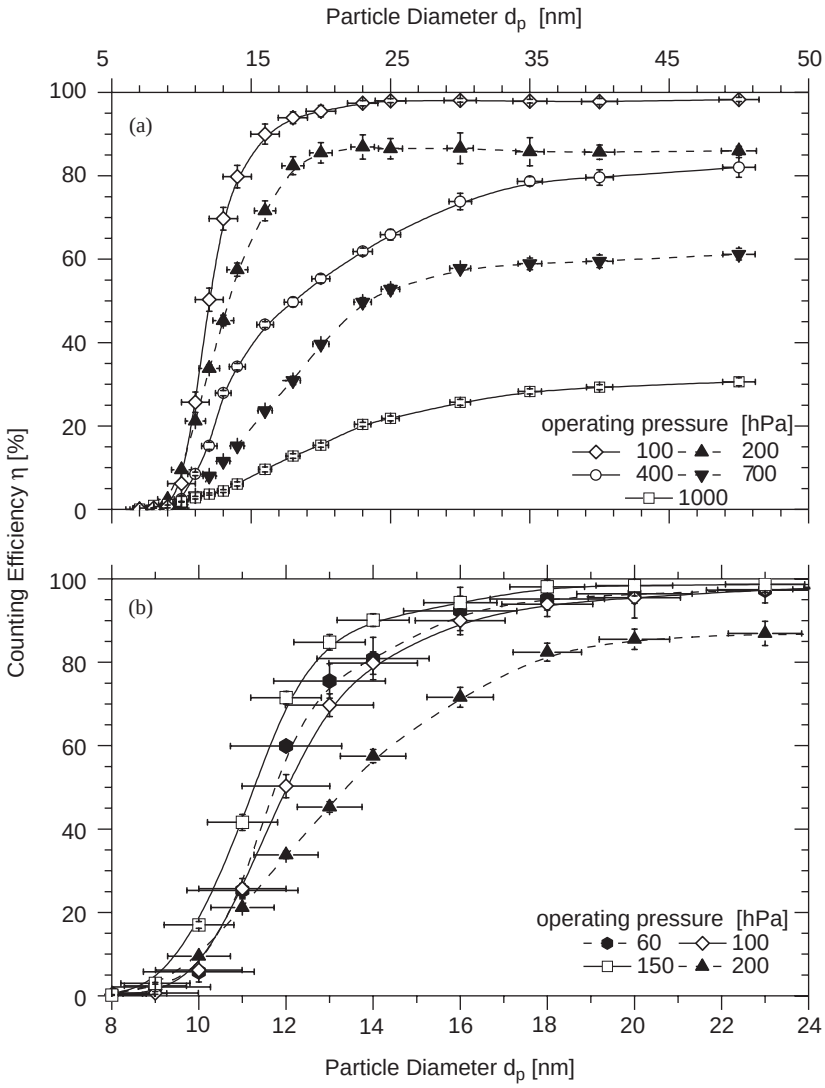

Fig. 2. CPC 7610 counting efficiency at operating pressures of 60, 100, 150, 200, 400, 700, and 1000 hPa. All curves were obtained using NaCl particles. Error bars on the x-axis represent the half-width of DMA-transfer window; y-axis error bars indicate the standard deviation of the mean values.

particles. As expected, the CPC 7610 shows a strong dependence on the temperature difference inside the instrument. With increasing temperature difference the counting efficiency curve shifts towards smaller diameters and concurrently the maximum counting efficiency increases. These changes can be explained by the higher supersaturations achieved in the condenser and were also found in previous studies (e.g., McDermott, Ockovic, & Stolzenburg, 1991; Mertes, Schröder, & Wiedensohler, 1995; Russell et al., 1996; Wiedensohler et al., 1997; Schröder & Ström, 1997; Hermann & Wiedensohler, 2001). The influence of the temperature difference on the counting efficiency curve increases as the pressure increases, as it can

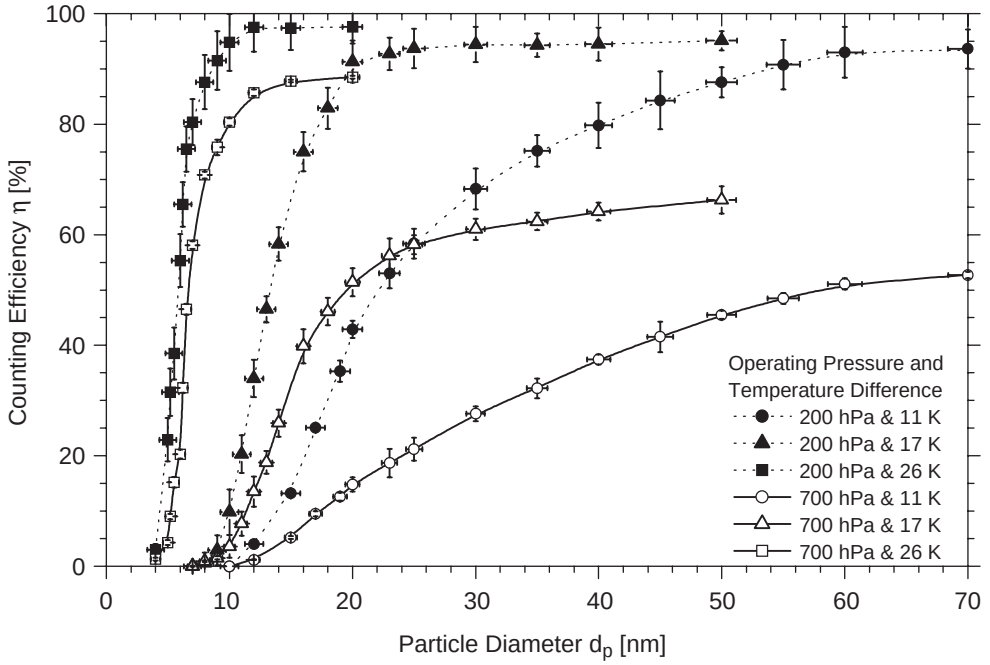

Fig. 3. CPC 7610 counting efficiency for 11, 17, and 26 K temperature difference at 200 and 700 hPa operating pressure, respectively. All curves were obtained using a H_2SO_4 particles.

be seen by comparing the 200 and 700 hPa curves. Again, an explanation for this behaviour will be given in Section 4.4.

4.3. Aerosol particle material dependence

Counting efficiency curves of CPCs operated with butanol show a small but significant dependence on aerosol particle material (cf. e.g., Hermann & Wiedensohler, 2001 and references therein). In this study, CPC 7610 calibration runs were performed with two different aerosol materials, NaCl and H_2SO_4, in order to investigate if FC-43 also shows this dependence. The respective counting efficiency curves for 200 and 1000 hPa are displayed in Fig. 4. The temperature difference was again 17 K. For 11 and 26 K, the graphs show the same behaviour. At 200 hPa, there is no difference visible in the lower threshold diameter, but the maximum counting efficiency for NaCl is lower by approximately 10%. Towards higher pressures, H_2SO_4 shows not only the higher maximum counting efficiency, but also the much lower threshold diameter. This indicates a dependence of the counting efficiency on particle material, which becomes larger as the pressure is increased. A reason for this dependence is not obvious. However, this difference cannot be explained by the particle shape alone, i.e., the fact that the NaCl particles are cubes and the H_2SO_4 particles are spheres (cf. Kelly & McMurry, 1992), which would lead to much smaller differences on the order of 10% in diameter. The results shown here are in contradiction to results obtained by Brock et al. (2000), who used the same particle materials but did not observe any difference in the sensitivity of FC-43.

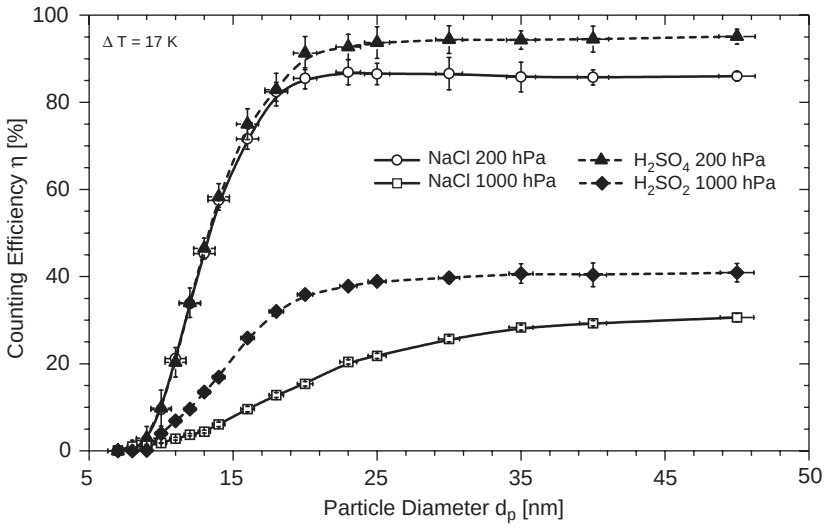

Fig. 4. CPC 7610 counting efficiency for NaCl and H_2SO_4 particles at 200 and 1000 hPa operating pressure, respectively, and 17 K temperature difference.

4.4. Comparison FC-43 and butanol

In Fig. 5, the counting efficiency curves of the CPC 7610 with FC-43 are compared to those measured with the original working fluid butanol (Hermann & Wiedensohler, 2001). For simplicity, the error bars (given in Fig. 2 and Hermann & Wiedensohler (2001)) were left out. All curves were taken at the standard temperature difference of 17 K. The FC-43 curves were obtained with NaCl particles, whereas the butanol curves were measured with Ag particles. These different particle materials induce a slight inconsistency when interpreting the curves, because the response of a CPC can be different for different particle materials (cf. Section 4.3). However, the shift in the lower threshold diameter between Ag- and NaCl-curves is small for butanol, on the order of 1–2 nm only, as shown in the literature (cf. Hermann & Wiedensohler, 2001 and references therein). The counting efficiency curves for different working fluids in Fig. 5 show, however, much larger differences. From 1000 hPa down to 200 hPa butanol shows the smaller threshold diameter and the higher maximum counting efficiency compared to FC-43. Furthermore, the butanol curves are less sensitive regarding pressure changes, which can occur e.g., in aircraft applications during ascents and descents. The counting efficiencies of both fluids become comparable at about 200 hPa. At lower pressures, the butanol curves begin to shrink (higher threshold diameters and lower maximum counting efficiencies) as the pressure decreases further and below 160 hPa a strong decrease in the instrument performance is observed (cf. Hermann & Wiedensohler, 2001, Fig. 4). Hence, below this pressure limit, the CPC 7610 is not applicable with butanol. FC-43, on the other hand, reaches its lowest threshold diameter and highest maximum counting efficiency in the pressure range below 200 hPa (cf. Fig. 2). It can be used at least down to 60 hPa. Note that the lowest pressure of 60 hPa investigated in this study was not determined by the instruments performance but rather by the limitation of the calibration set-up, e.g., the suction power of the pump. In summary, using the CPC 7610 with the original flow rate, FC-43 can be recommended for applications with operating pressures below 200 hPa (e.g., for measurements in the stratosphere), whereas above this threshold value butanol yields the more stable counting efficiency

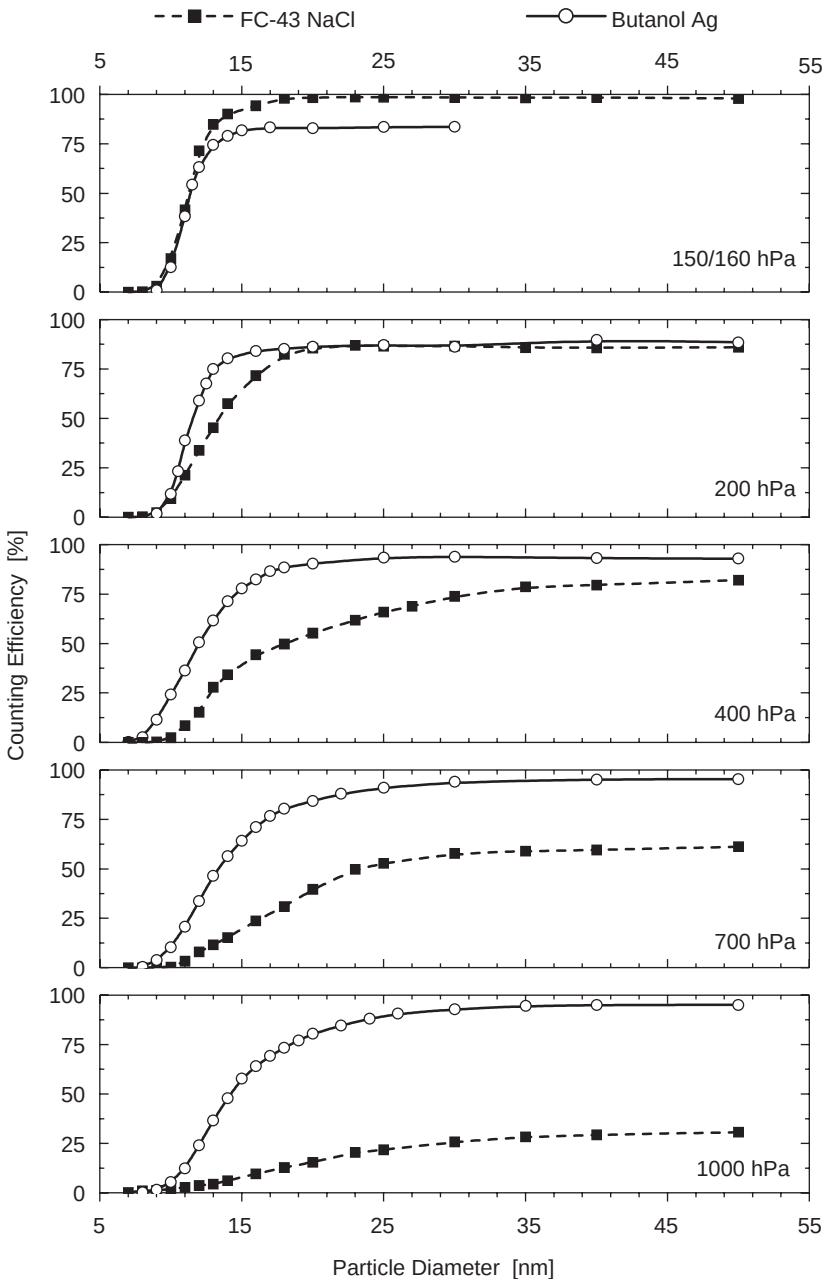

Fig. 5. CPC 7610 counting efficiency at various pressures for the working fluids butanol and FC-43, respectively. Temperature difference was set to 17 K. FC-43 curves were obtained using NaCl particles. The butanol curves were taken from Hermann and Wiedensohler (2001) and were measured with Ag particles. In the uppermost graph the butanol curve corresponds to 160 hPa, whereas the FC-43 curve was measured at 150 hPa.

curves with lower threshold diameters and higher maximum counting efficiencies. For other CPC types the picture should be similar, however, they probably have a different threshold pressure value.

Looking at the experimental results for FC-43 and 1000 hPa, an obvious question is: Why are particles as large as 50 nm counted with a maximum counting efficiency of only ∼ 30%? In principle, activation for such relatively large particles should not be a problem. In order to explain this difference to butanol, we applied CFD modelling to describe the working fluid mass transfer inside the CPC saturator (cf. Section 3). As result, Fig. 6 shows the FC-43 saturation for six different pressures at the CPC 7610 saturator exit plane, where the aerosol flow leaves the saturated sponge. Besides the fact that the flow pattern is changing with pressure, the striking features of this figure are that at ambient pressure the sampling air is not saturated with FC-43 and not until 150 hPa "full" saturation is achieved all over the saturator exit plane. The minimum and the mean saturation values for 1000 hPa are only 25% and 54%, respectively, but they reach 92% and 97% at 150 hPa. This subsaturation is due to the relatively small diffusion coefficient of FC-43 (cf. Table 1), which increases with decreasing pressure. As there are only a few regions of the saturator exit plane where high saturation values are reached for ambient pressure, there are likewise only a few regions in the condenser where the supersaturation is high enough to activate particles. This is most likely the explanation for the decreasing maximum counting efficiency with increasing pressure observed for FC-43 (cf. Section 4.1). Furthermore, this effect also explains that the influence of the temperature difference on the counting efficiency curve increases as the pressure increases (cf. Section 4.2). At higher pressures, the saturation and hence the FC-43 vapour pressure at the saturator exit plane is lower, as the model results show. In the condenser, the lower vapour pressure values lead to lower supersaturations, which are more sensitive to the CPC temperature difference. In order to improve the CPC performance with FC-43 one would have to lengthen the saturator or to reduce the flow rate through the instrument.

In contrast to FC-43, butanol has a three times larger diffusion coefficient (cf. Table 1). Consequently, the butanol saturation at the saturator exit plane should be higher at any pressure compared to FC-43. This is shown in Fig. 7 for 1000 and 400 hPa, where the mean butanol saturation is already 75% and 93%, compared to 54% and 74% for FC-43, respectively. This explains the higher maximum counting efficiencies for butanol. Even for butanol the performance of the CPC could be improved by lengthening the saturator (as implemented in the improved CPC Model 7620/3761) or by reducing the flow rate.

In Fig. 8, we plotted the maximum experimental asymptotic counting efficiency for three CPC temperature differences versus the modelled mean FC-43 saturation at the saturator exit plane. The three data points to the left belong to the 1000 hPa model case, and moving to the right, the 700, 400, 200, 150, and 100 hPa data points follow, if available. The plot shows that there is a clear correlation between the saturation and the maximum counting efficiency, emphasising the above statements. Furthermore, by extrapolating the three curves, it is found that at least ∼ 50% FC-43 saturation at the saturator exit plane is needed in order to count any particles with the CPC 7610.

4.5. Threshold diameters and maximum counting efficiencies

To summarise the FC-43 calibration measurements, all counting efficiency curves were fitted using a four-parameter exponential function given by Wiedensohler et al. (1997):

$$\begin{aligned} &\eta = \eta_{\max} - a\left(1 + \exp\left(\frac{d_p - b}{c}\right)\right)^{-1} && \text{for } d_p \geqslant d_0, \\ &\eta = 0, && \text{for } d_p < d_0, \end{aligned} \tag{1}$$

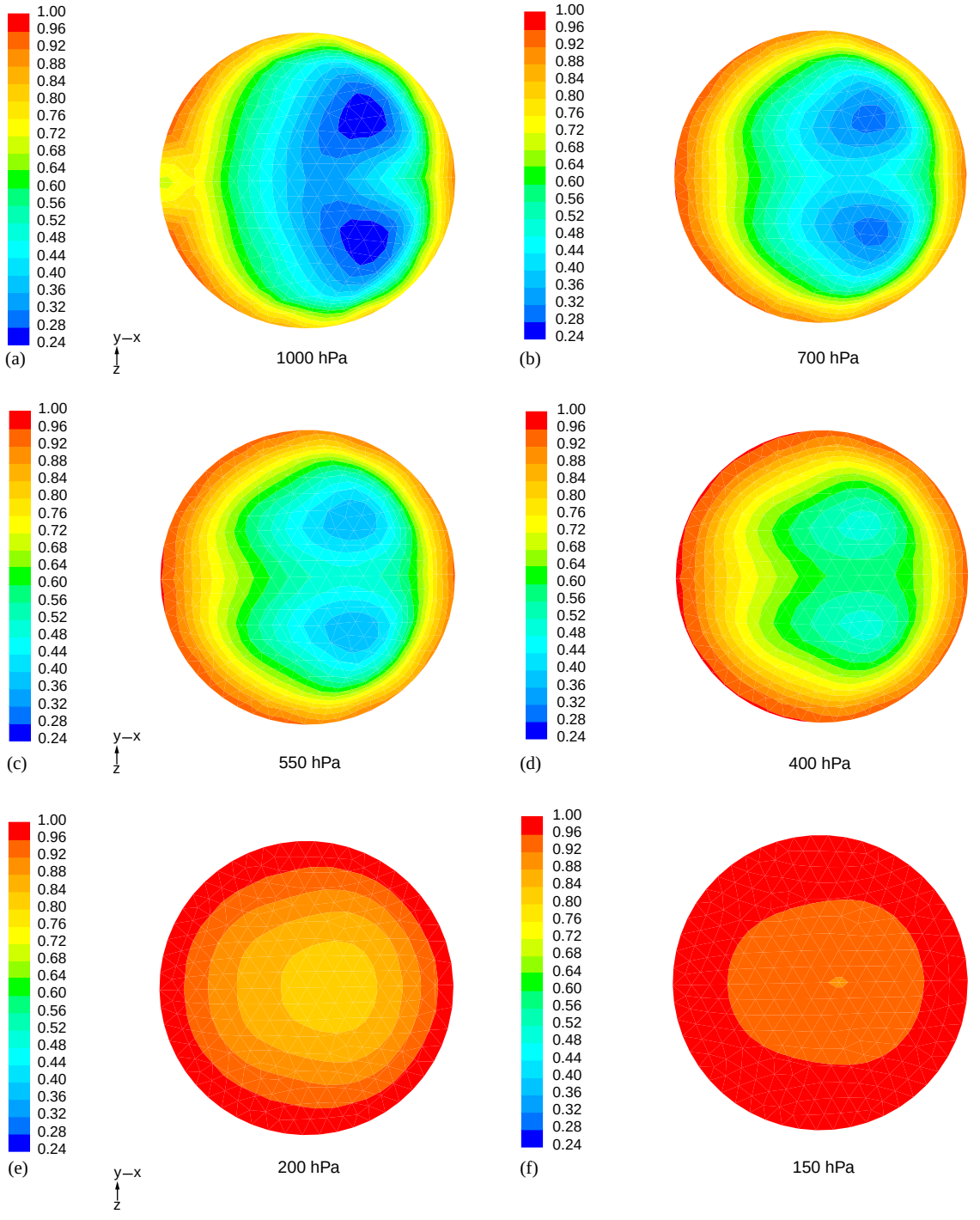

Fig. 6. FC-43 saturation at the CPC 7610 saturator exit plane. The non-symmetric features in the contours are caused by the saturator geometry (e.g., nozzle-like geometry and 90°bend upstream the saturator exit plane).

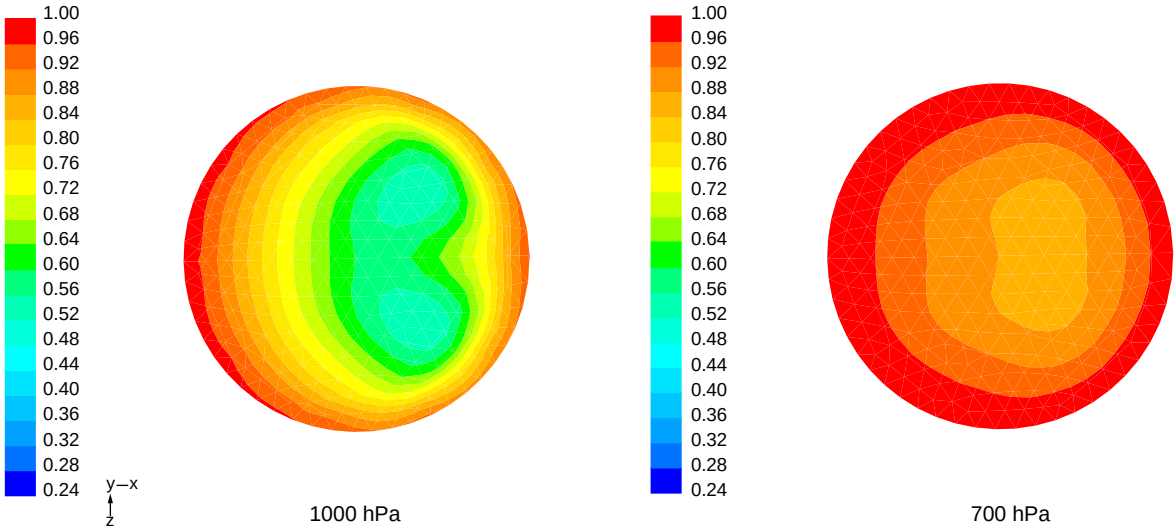

Fig. 7. Butanol saturation at the CPC 7610 saturator exit plane.

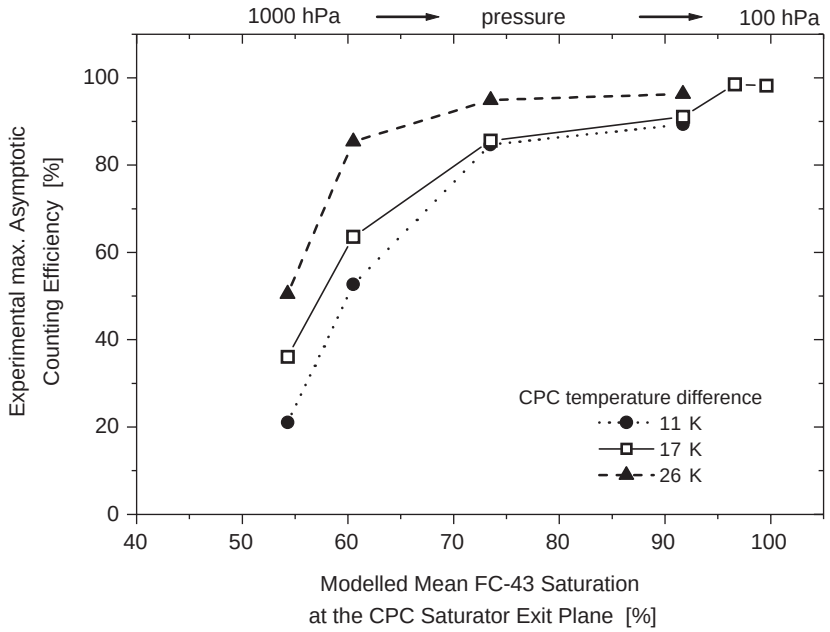

Fig. 8. Maximum asymptotic counting efficiencies η_{max} as function of mean modelled FC-43 saturation at the saturator exit plane. Left-most data points belong to the highest operating pressure (1000 hPa), and moving to the right, the 700, 400, 200, 150, and 100 hPa data points follow.

Table 2
Threshold diameters dp_{50} for the CPC 7610 operated with FC-43

d_{p50}	NaCl			H_2SO_4		
Pressure	ΔT (K)			ΔT (K)		
(hPa)	11	17	26	11	17	26
60		11.7				
100		12.0				
150		11.2				
200	27.0	12.8	5.9	22.0	13.1	5.8
400	39.2	16.4	5.9	26.8	15.5	5.5
700	35.1	17.6	6.4	31.3	15.2	6.6
1000	38.8	20.1	6.6	41.6	14.7	6.7

Volume flow rate was 1.1–1.6 l/min (pressure-dependent, cf. Hermann & Wiedensohler, 2001). Data were calculated using the fitting function Eq. (1).

Table 3
Maximum asymptotic counting efficiencies η_{max} for the CPC 7610 operated with FC-43

η_{max}	NaCl			H_2SO_4		
Pressure	ΔT (K)			ΔT (K)		
(hPa)	11	17	26	11	17	26
60		98.3				
100		98.2				
150		98.5				
200	84.9	86.9	94.8	93.7	95.2	97.8
400	82.6	84.0	91.8	86.8	87.2	98.0
700	51.8	61.1	82.0	58.3	66.0	88.8
1000	16.5	31.1	48.3	25.4	41.0	52.8

Volume flow rate was 1.1–1.6 l/min. Data were calculated using the fitting function Eq. (1).

$$\text{with } d_0 = c \ln\left(\frac{a}{\eta_{max} - 1}\right) + b.$$

Using this fitting function, the threshold diameters of the 50% particle detection efficiency, d_{p50} were calculated. In this context, the d_{p50} was defined as particle diameter where the counting efficiency reaches half the maximum asymptotic counting efficiency η_{max}. The resulting d_{p50} and η_{max} values are listed in Tables 2 and 3, respectively, which summarise the results from the figures given above. The numbers show clearly that the CPC 7610 operated with FC-43 has its best performance at low pressures and high temperature differences. For some temperature set-ups a smaller d_{p50} is calculated as the pressure increases, e.g., for the 17 K temperature difference curve and sulphuric acid particles. However, this "trend" is only caused by the rapid decrease in η_{max} and the used definition of the d_{p50} and not by a better instrument performance.

5. Summary

In this study, the counting efficiency of the TSI CPC 7610 operated with FC-43 as working fluid was investigated. Counting efficiency curves were measured for three temperature differences (11, 17, and 26 K) in the pressure range from 60 to 1000 hPa. In general, the CPC 7610 counting efficiency increases as the operating pressure is decreased or the temperature difference is increased. At the standard temperature difference of 17 K, the CPC threshold diameter decreases from $\sim$ 20 to $\sim$ 11.5 nm and the maximum counting efficiency increases from $\sim$ 30% to $\sim$ 100% as the operating pressure is reduced from 1000 hPa down to 60 hPa. For NaCl and H_2SO_4 particles, the CPC 7610 operated with FC-43 shows different counting efficiency curves. Hence, the condensation process of FC-43 seems to be sensitive to particle material, similar to butanol, but even stronger. Comparison with the counting efficiency curves obtained with butanol as working fluid shows that above 200 hPa butanol yields the more stable counting efficiency curves (less sensitive to pressure changes) with lower threshold diameters and higher maximum counting efficiencies. However, below 200 hPa, FC-43 yields the better performance and can be used down to at least 60 hPa.

In order to explain the differences in the maximum counting efficiency between FC-43 and butanol, we modelled the working fluid mass transfer inside the CPC 7610 saturator using a CFD code (FLUENT). The results show that due to the relative small diffusion coefficient of FC-43, the mean FC-43 saturation at the saturator exit plane is only 54% for 1000 hPa and does not reach 100% until approximately 150 hPa. These low saturation values lead to smaller supersaturation values in the CPC condenser block, and consequently a smaller fraction of particles is activated and counted. This is emphasised by a clear correlation between the maximum counting efficiency and the mean saturation at the saturator exit plane.

The next step of analysis would be to model the particle activation and growth in the CPC condenser block. However, as the CPC 7610 condenser geometry is quite complex and calculations of particle dynamic processes lead to additional equations, which have to be solved, this would require a full 3D model of the CPC and time consuming calculations. Furthermore, as the real wall temperature distribution of the condenser block is not known, but the model results are quite sensitive to this parameter, the large degree of uncertainty of this boundary condition could lead to uncertain results. However, for simpler CPC geometries or other applications with well defined boundary conditions the combination of FLUENT with the FPM, (www.particle-dynamics.de) will be a useful tool to characterise particle instruments and systems in the future.

References

Adler, S., (2003). Untersuchung der Funktionsfähigkeit von Kondensationspartikelzählern mit FC-43 als Arbeitssubstanz. MSc. Thesis, Westsächsische Hochschule Zwickau (FH), Germany.

Brock, C. A., Schröder, F., Kärcher, B., Petzold, A., Busen, R., & Fiebig, M. (2000). Ultrafine particle size distributions measured in aircraft exhaust plumes. *Journal of Geophysics Research*, *105*(26), 555–567.

Fuller, E. N., Ensley, K., & Giddings, J. C. (1969). Diffusion of halogenated hydrocarbons in helium: the effect of structure on collision cross sections. *Journal of Physical Chemistry*, *73*, 3679.

Fuller, E. N., & Giddings, J. C. (1965). A comparison of methods for predicting gaseous diffusion coefficients. *Journal of Gas Chromatography*, *3*, 222.

Fuller, E. N., Schettler, P. D., & Giddings, J. C. (1966). A new method for the prediction of binary gas-phase diffusion coefficients. *Industrial Engineering Chemical*, *58*(18),

Hanson, D. R., Eisele, F. L., Ball, S. M., & McMurry, P. M. (2002). Sizing small sulfuric acid particles with an ultrafine particle condensation nucleus counter. *Aerosol Science and Technology*, *36*, 554–559.

Hermann, M., & Wiedensohler, A. (2001). Counting efficiency of condensation particle counters at low-pressures with illustrative data from the upper troposphere. *Journal of Aerosol Science*, *32*, 975–991.

Joback, K. G., & Reid, R. C. (1987). Estimation of pure-component properties from group-contributions. *Chemical Engineering Communications*, *57*, 233–243.

Keady, P. B., Denler, V. L., Sem, G. J., Stolzenburg, M. R., & McMurry, P. H., (1988). A condensation nucleus counter designed for ultrafine particle detection above 3 nm diameter. *Atmospheric aerosols and nucleation*. *Proceedings*, *12th international conference on atmospheric aerosols and nucleation*. Vienna, Austria, 22–27.

Kelly, W. P., & McMurry, P. H. (1992). Measurement of particle density by inertial classification of differential mobility analyzer-generated monodisperse aerosols. *Aerosol Science and Technology*, *17*, 199–212.

Lucas, K., (1984). VDI-Wärmeatlas, Abschnitt DA. Berechnungsmethoden für Stoffeigenschaften. Verein Deutscher Ingenieure. Düsseldorf, Springer.

McDermott, W. T., Ockovic, R. C., & Stolzenburg, M. R. (1991). Counting efficiency of an improved 30 Å condensation nucleus counter. *Aerosol Science and Technology*, *14*, 278–287.

Mertes, S., Schröder, F., & Wiedensohler, A. (1995). The particle detection efficiency curve of the TSI 3010 CPC as a function of the temperature difference between saturator and condenser. *Aerosol Science and Technology*, *23*, 257–261.

Particle Dynamics, (2003). FPM-1.0.1 users guide. Particle dynamics GmbH Leipzig, Germany.

Roy, D., & Thodos, G. (1968). *Industrial and Engineering Chemistry Fundamentals*, *7*, 529.

Roy, D., & Thodos, G. (1970). *Industrial and Engineering Chemistry Fundamentals*, *9*, 71.

Russell, L. M., Zhang, S.-H., Flagan, R. C., Seinfeld, J. H., Stolzenburg, M. R., & Caldow, R. (1996). Radially classified aerosol detector for aircraft-based submicron aerosol measurements. *Journal of Atmosphere and Oceanic Technology*, *13*, 598–609.

Saros, M. T., Weber, R. J., Martri, J. J., & McMurry, P. H. (1996). Ultrafine aerosol measurement using a condensation particle counter with pulse height analysis. *Journal of Aerosol Science*, *25*, 200–213.

Scheibel, H. G., & Porstendörfer, J. (1983). Generation of monodisperse Ag- and NaCl-aerosols with particle diameters between 2 and 300 nm. *Journal of Aerosol Science*, *14*, 113–126.

Schröder, F., & Ström, J. (1997). Aircraft measurements of sub micrometer aerosol particles (>7 nm) in the midlatitude free troposphere and tropopause region. *Atmosphere Research*, *44*, 333–356.

Seto, T., Nakamoto, T., Okuyama, K., Adachi, M., Kuga, Y., & Takeuchi, K. (1997). Size distribution measurement of nanometer-sized aerosol particles using DMA under low pressure conditions. *Journal of Aerosol Science*, *28*, 193–206.

Stolzenburg, M.R., (1988). *An ultrafine aerosol size distribution measuring system*. Ph.D. Thesis, Mechanical Engineering Department, University of Minnesota, Minneapolis, USA.

Wiedensohler, A., Orsini, D., Covert, D. S., Coffmann, D., Cantrell, W., Havlicek, M., Brechtel, F. J., Russell, L. M., Weber, R. J., Gras, J., Hudson, J. G, & Litchy, M. (1997). Intercomparison study of the size-dependent counting efficiency of 26 condensation particle counters. *Aerosol Science and Technology*, *27*, 224–242.

Wilck, M., Stratmann, F., & Whitby, E.R., (2002). A fine particle model for fluent: description and applications. *Presentation at the sixth international aerosol conference (IAC 2002)*. Taipei, Taiwan, 8–13 September.

Willeke, K., Baron, P. A., (2001). *Aerosol measurements*: *principles techniques and applications*. New York: Wiley, 1131pp.